

Sensitive disk resonator photonic biosensor

Robert W. Boyd and John E. Heebner

We describe a photonic device based on a high-finesse, whispering-gallery-mode disk resonator that can be used for the detection of biological pathogens. This device operates by means of monitoring the change in transfer characteristics of the disk resonator when biological materials fall onto its active area. High sensitivity is achieved because the light wave interacts many times with each pathogen as a consequence of the resonant recirculation of light within the disk structure. Specificity of the detected substance can be achieved when a layer of antibodies or other binding material is deposited onto the active area of the resonator. Formulas are presented that allow the sensitivity of the device to be quantified and that show that, under optimum conditions, as few as 100 molecules can be detected.

© 2001 Optical Society of America

OCIS codes: 170.4580, 230.3990.

1. Introduction

There is great need for highly sensitive techniques for the detection of trace amounts of biological pathogens.¹ In the laboratory, standard spectroscopic techniques² can be used to detect various biological materials with great sensitivity and specificity, but for use outside of a laboratory environment there is great need for robust, integrated devices that are both inexpensive and can be used in harsh environments. Integrated optics or photonics allow optobiological interactions in a compact geometry. Some techniques that are under intense investigation include biosensors constructed from directional couplers,³ Mach-Zehnder interferometers,⁴ and various configurations that make use of surface-plasmon resonance.⁵⁻⁷

In this paper we analyze use of high-finesse, microcavity devices to construct high-sensitivity biosensors. Microresonators have previously found application in disk lasers,⁸⁻¹¹ high-resolution spectroscopy,¹² laser frequency stabilization,¹³ add-drop filters for wavelength division multiplexing,¹⁴ dispersion compensation,¹⁵ all-optical switching,^{16,17} and cavity quantum electrodynamics.¹⁸⁻²⁰ Moreover, Blair and Chen²¹ have recently proposed use of cy-

lindrical optical cavities for resonantly enhanced fluorescence biosensing. In the present paper we describe an alternative procedure based on absorption for performing high-sensitivity detection of biological materials and present an analysis of the limiting sensitivity that can be achieved through use of such a device. In particular, the device described here differs from that of Blair and Chen in that they propose use of microresonators to enhance the intensity of the fluorescence emitted by biological materials, whereas we propose monitoring the transfer characteristics (for example, the transmission) of a microresonator to detect trace amounts of biological material on the surface of the microresonator.

The technique described in this manuscript is based on use of the device shown schematically in Fig. 1(a). Here light from an optical waveguide is allowed to excite a whispering-gallery mode^{8,9,22,23} of a disk resonator. The spacing between the waveguide and the resonator is adjusted so that the coupling between the two is weak, which allows the light intensity to build up to high values within the resonator. We define the ratio of the circulating intensity within the resonator to the incident intensity to be the buildup factor B of the configuration.²⁴ In use, biological materials are allowed to fall onto the region of the disk where the light is confined, and the presence of these materials is detected when the change in the transfer characteristics of the resonator is monitored. We show in Section 4 that the sensitivity to detect the presence of absorbing species is increased with respect to direct detection by the buildup factor of the structure, which in a well-designed device can probably be as large as 10^4 .²⁵

The authors are with the Institute of Optics, University of Rochester, Rochester, New York 14627. R. W. Boyd's e-mail address is boyd@optics.rochester.edu.

Received 7 May 2001; revised manuscript received 1 August 2001.

0003-6935/01/315742-06\$15.00/0

© 2001 Optical Society of America

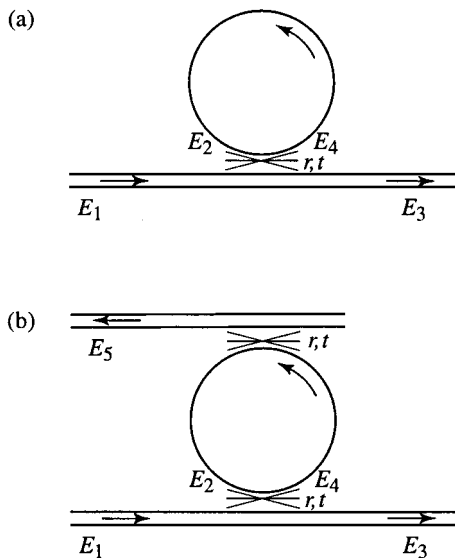


Fig. 1. (a) Geometry of the biosensor. Light from an optical waveguide is weakly coupled (with coupling coefficients r and t) to a whispering-gallery mode of a high-finesse disk resonator. The presence of biological materials near the surface of the disk leads to a dramatic change in the transfer characteristics of the device. (b) Alternative design of the biosensor that could be used to monitor the presence of biological materials through an induced change in the refractive index of the disk material.

Such a device could be constructed by means of known fabrication techniques.²⁶ At present, many single microresonator systems with excellent optical properties have been constructed.^{27–30} In many of these cases, extending the fabrication techniques to construct long sequences of such devices to yield large-scale integration of photonic microresonators³¹ is achievable, with the potential for construction of arrays of biosensors of the type shown in Fig. 1(a), each of which could, for example, be sensitized with a different antibody layer.

We conclude this introduction with a brief description of some recent research that is related to our proposed device. Hall and Pollard² consider use of the near-IR spectral region for the analysis of biological materials. They show (see especially their Figs. 1 and 2) that they can discriminate among various serum specimens (in particular, clear serum, hemolyzed serum, lipemic serum, and jaundiced serum) by means of their absorption spectra. They obtained the greatest sensitivity in the visible (400–700-nm region), but also found discrimination in the water overtone band region (around 1450 nm) and the combination band region (around 1940 nm). Use of the near-IR spectral region for the design of photonic biosensors is quite attractive from a fabrication point of view because of the knowledge base of techniques developed by the telecommunications industry.

Salmaso *et al.*³² studied the optical properties of eosinophilic granulocytes. They concluded that the optical properties are primarily those of eosinophil peroxidase and present an absorption spectrum (their Fig. 1) that shows a strong feature at 400 nm

and a weaker feature at 650 nm. Luff *et al.*³ described a biosensor that utilizes a 633-nm laser. It has the configuration of a directional coupler and operates by detecting the change in refractive index when biological materials fall onto the sensor element. They present data (their Fig. 5) showing that they can detect the presence of a single layer of biological material. They deposit alternating layers of biotinylated bovine serum albumin and polystyrene. In later research, Luff *et al.*⁴ described a biosensor with similar sensitivity having the form of a Mach-Zehnder interferometer that operates at 786 nm.

Kolomenskii *et al.*^{6,7} described a biosensor based on surface-plasmon resonance. The device they built operates at 633 nm and works by detecting the change in reflectivity near the single-plasmon resonance angle. They used this device to measure the concentration of Rhodamine 700 in ethanol. They also used this device to detect the presence of the protein bovine serum albumin by a process in which they immobilized the bovine serum albumin molecule by binding to a carboxymethylated dextran layer. In summary, several techniques have been successfully demonstrated for the construction of photonic biosensors in the visible and near-IR spectral regions. It is hoped that biosensors of the type described here that are based on the properties of disk microresonators can provide superior sensitivity because of the potentially large values of the enhancement factor B associated with the recirculation of light within the resonator structure.

2. Mathematical Model

We analyze mathematically the device illustrated in Fig. 1 as follows.³³ We describe the coupling of light into and out of the resonator in terms of generalized beam-splitter relations of the form

$$E_3 = rE_1 + itE_2, \quad (1)$$

$$E_4 = rE_2 + itE_1, \quad (2)$$

where r and t are taken to be real quantities that satisfy the relation $r^2 + t^2 = 1$ and where the fields are defined with respect to the reference points indicated in Fig. 1. In addition, we describe the circulation of light within the resonator in terms of the round-trip phase shift ϕ and the amplitude transmission factor τ such that

$$E_2 = \tau \exp(i\phi) E_4. \quad (3)$$

The round-trip phase shift ϕ can be interpreted as kL_{eff} , where $k = 2\pi n/\lambda$, n is the effective refractive index of the disk structure, λ is the vacuum wavelength of the incident light, and L_{eff} is the effective circumference of the mode of the disk resonator, which is roughly equal to the physical circumference of the disk. The disk is assumed to be constructed of lossless materials. The transmission can be smaller than unity as the result of the absorption by biological materials located near the resonator structure or

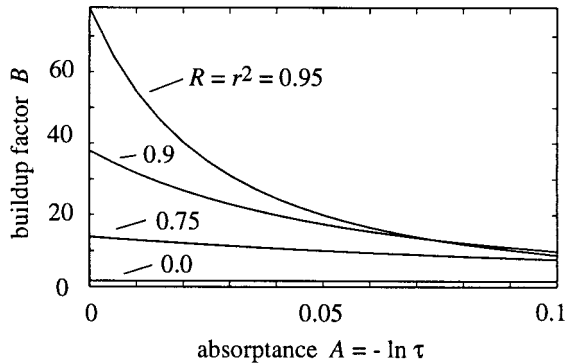


Fig. 2. Buildup factor B for the device shown in Fig. 1(a) plotted against the single-pass absorption $A = -\ln \tau$ for several values of the coupling coefficient $R = r^2$.

due to unwanted losses associated with poor confinement of light³⁴ within the resonator. Equations (1)–(3) can be solved simultaneously to find that the input and output fields are related by

$$\frac{E_2}{E_1} = \frac{it\tau \exp(i\phi)}{1 - r\tau \exp(i\phi)}. \quad (4)$$

The absolute square of this quantity is the buildup factor B introduced above:

$$B = \frac{I_2}{I_1} = \left| \frac{E_2}{E_1} \right|^2 = \frac{(1 - \tau^2)\tau^2}{1 - 2r\tau \cos(\phi) + r^2\tau^2}. \quad (5)$$

It should be noted that the buildup takes on its maximum value

$$B_{\max} = \frac{1 + \tau}{1 - r} \quad (6)$$

under conditions such that the incident light is resonant with the structure (that is, $\phi = 2\pi m$ for integral m) and attenuation is negligible ($\tau = 1$). We next determine the transmission through the waveguide that is coupled to the disk resonator. We find the amplitude transmission E_3/E_1 by combining Eqs. (1) and (4) to obtain

$$\frac{E_3}{E_1} = \exp[i(\pi + \sigma)] \frac{\tau - r \exp(-i\phi)}{1 - r\tau \exp(i\phi)}. \quad (7)$$

The intensity transmission factor T is given by the squared modulus of this quantity or by

$$\frac{I_3}{I_1} = \left| \frac{E_3}{E_1} \right|^2 = \frac{\tau^2 - 2r\tau \cos \phi + r^2}{1 - 2r\tau \cos \phi + r^2\tau^2}. \quad (8)$$

3. Predictions of the Model

Some of the predictions of the model just presented are shown in Figs. 2–4. Figure 2 shows how the buildup factor B depends on the presence of absorption occurring within the resonator structure. The buildup factor is plotted against the single-pass absorption A , defined in terms of the single-pass transmission such that $\tau^2 = \exp(-A)$, and results are

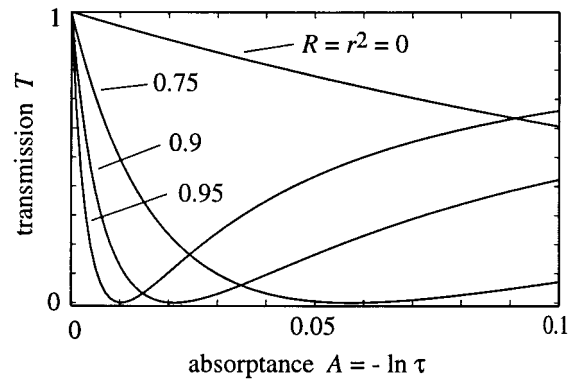


Fig. 3. Resonator transmission $T = |E_3/E_1|^2$ for the device shown in Fig. 1(a) plotted against the single-pass absorption $A = -\ln \tau$ for several values of the coupling coefficient $R = r^2$.

shown for several values of the coupling coefficient $R = r^2$. One can see that, for coupling coefficients R approaching unity, the buildup factor B decreases rapidly with increasing absorption. This variation of the internal intensity with the internal absorption A can be monitored in any of several different ways to form a biosensor. For example, one can measure the intensity of inevitable scattering of light out of the resonator to monitor the intensity of the circulating light. Alternatively, one can measure the intensity of the light leaving the output port of the device. This possibility is analyzed next.

Figure 3 shows how the transmitted intensity varies with the presence of internal absorption within the disk resonator. More precisely, the resonator transmission $T = |E_3/E_1|^2$ is plotted against the single-pass absorption $A = -\ln \tau$ for several values of the coupling coefficient $R = r^2$. Note that in all cases the device transmission initially decreases with increasing absorption and that for some particular value of the absorption the transmission drops to zero. Under these conditions, the resonator is said to be critically coupled to the optical waveguide. The vanishing of the transmission can be traced to a complete destructive interference of the two contributions [see Eq. (1)] to the transmitted field. Either of these properties can be used to construct a biosensor. For example, examination of Eq. (8) shows that the transmission drops to zero when the absorption has the value

$$A = -\ln R. \quad (9)$$

In addition, one can easily show that the change in transmission with absorption is maximum for small absorption under resonance conditions and has the value

$$dT/dA = B, \quad (10)$$

where B is the buildup factor introduced above.

It is also possible to construct a biosensor based on the change in phase of the circulating optical power resulting from the change in refractive index of the disk when biological materials fall onto its surface.

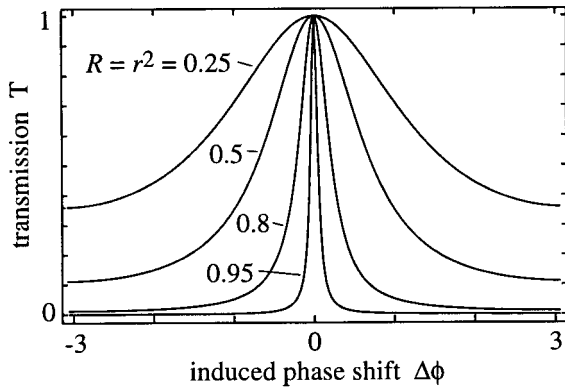


Fig. 4. Resonator transmission $T = |E_3/E_1|^2$ plotted against the single-pass phase shift $\Delta\phi$ for several values of the coupling coefficient $R = r^2$ for the balanced, four-port device shown in Fig. 1(b).

A device that could function in this manner is shown in Fig. 1(b); it is a variation of the device in Fig. 1(a) in that the disk resonator is coupled to two separate waveguides. Two output ports are required in this case because, in the absence of absorption, the transmission of the device of Fig. 1 is equal to unity for any value of the single-pass phase ϕ as a result of energy conservation. For the two-output-port device of Fig. 1(b), the input power is split between the two output ports in a manner that depends on the phase ϕ . A simple calculation analogous to that of Section 2 shows that the transmission functions for this device are given in the absence of absorption by

$$\begin{aligned}
 T_5 &= \frac{I_5}{I_1} \\
 &= \frac{(1 - r^2)^2}{1 - 2r^2 \cos \phi + r^4} \\
 &= \frac{1}{1 + \frac{4r^2}{(1 - r^2)^2} \sin^2 \frac{1}{2} \phi}, \quad (11)
 \end{aligned}$$

$$T_3 = \frac{I_3}{I_1} = 1 - T_5. \quad (12)$$

Equations (11) and (12) are a form of the Airy formula, which is encountered in the theory of the Fabry–Perot interferometer. Shown in Fig. 4 is a plot of the resonator transmission $T = |E_3/E_1|^2$ against the single-pass phase shift $\Delta\phi$ for several values of the coupling coefficient $R = r^2$. These curves were calculated under the assumption that the coupling coefficient was the same for the two waveguides. We can see that, as the coupling coefficient R approaches unity, the central resonance becomes sharp. The extremely sensitive dependence of the transmission on the single-pass phase shift in this limit can be used to construct sensitive biosensors.

4. Sensitivity as a Biosensor

Let us next estimate the sensitivity of the device described above for the detection of biological substances. In practice, it is likely that a layer of biological material such as an antibody layer would be applied to the active area of the disk resonator of Fig. 1 to provide a specific binding of the type of material to be detected.^{3,4,6,7,35} For the present, we ignore the complications associated with the nature of this binding and, as a first approximation, estimate the minimum number of biological molecules that would have to fall onto the active area of the sensor to produce a reliable detection event. We note that the absorption cross sections of biological molecules are unlikely to change dramatically as a consequence of the weak (by chemical standards) binding associated, for example, with the binding of an antigen to an antibody. Thus the calculation presented here is likely to provide a reliable estimate of the sensitivity limits even in the more complicated situation in which a binding layer is employed. We take as a representative value of the absorption cross section of a biological molecule the value $\sigma = 2 \times 10^{-16} \text{ cm}^2$, the measured value for the substance dopamine.³⁶ One would expect that the absorption cross section for all single-electron, electric dipole transitions of molecules in the condensed phase would be of this order of magnitude. If \mathcal{A} is the cross-sectional area of the mode of the optical field that is excited within the disk resonator, the fraction of the light that is absorbed per pass in interacting with this molecule is $f = \eta\sigma/\mathcal{A}$. Here $\eta < 1$ is an efficiency factor that accounts for the fact that the molecule, located on the surface of the disk, does not experience the maximum intensity of the guided optical mode. We expect that \mathcal{A} would be of the order of $(\lambda/n)^2$, where n is the effective refractive index of the guiding region of the disk, and for $\eta = 0.5$ and $\lambda/n = 1 \text{ }\mu\text{m}$ we find that $f_{\text{abs}} = 1 \times 10^{-8}$. Such a small absorption is probably immeasurably small, but as noted above the total absorption is increased by the buildup factor B of the resonator, which could be as large as 10^4 .³⁷ Because a change in transmission of 1% is probably measurable, this calculation suggests that as few as 100 biological molecules falling onto the biosensor could produce a detection event.

It is also useful to deduce some general formulas relating to the sensitivity of the biosensor of Fig. 1. Equation (9) gives the condition under which the transmission of the sensor will drop to zero. We can express this result in terms of laboratory units as follows. Because $A = -\ln \tau$, where the single-pass transmission τ can be represented as $\tau = 1 - f_{\text{abs}}$, we find that for $f_{\text{abs}} \ll 1$ that $A \approx f_{\text{abs}}$. Furthermore, because for $R = r^2 \approx 1$, the buildup factor B of Eq. (5) is given by $B = 2/(1 - r)$, one finds that $R \approx 1 - 4/B$. Thus the condition of Eq. (9) to produce a strict zero in the sensor transmission can be expressed as

$$f_{\text{abs}} = \frac{4}{B}. \quad (13)$$

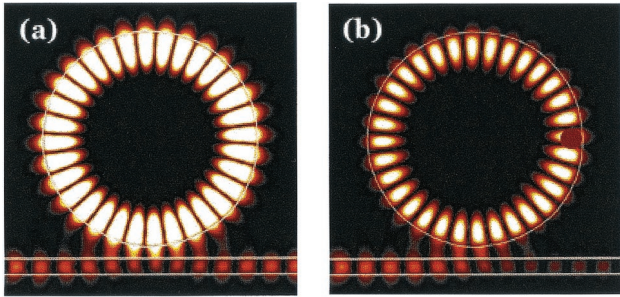


Fig. 5. Simulation of the field distribution in the region of the disk and waveguide, both in the (a) absence and (b) presence of an absorbing particle.

A more readily achieved condition is that the transmission through the device drops by a (smaller) prescribed amount. By means of a calculation analogous to that just presented, one finds that the amount of single-pass absorption required for the transmission to drop from unity to the value T (where it is assumed that $1 - T \ll 1$) is given by

$$f_{\text{abs}} = \frac{1 - T}{B}. \quad (14)$$

For definiteness, the discussion of the detection sensitivity given above was cast in terms of the minimum number of individual molecules that can give rise to a detection event. It should be noted that many biological materials possess an absorption cross section much larger than that of simple molecules such as dopamine, which was used in this calculation. For example, a macromolecule such as a polypeptide chain could readily contain more than 100 side-chain units each with an absorption cross section comparable to that of dopamine, and thus should be detected. Larger entities such as viruses should also be detectable.

5. Numerical Modeling of the Biosensor

We also modeled the operation of the device by performing a numerical integration of Maxwell's equations for a region of space that includes the disk resonator and a portion of the waveguide. An example of the results of such a simulation is shown in Fig. 5, which compares the field distribution both in the absence and presence of an absorbing biological pathogen. For the particular values of the parameters used in this calculation (see below), the presence of the pathogen leads to a dramatic change in the transmission characteristics of the device. In particular, in the presence of the pathogen the intensity of the circulating light field within the resonator decreases significantly and the transmitted intensity drops nearly to zero, illustrating the destructive interference mentioned in connection with Fig. 3.

The simulation shown in Fig. 5 was calculated through use of the finite-difference time-domain method³⁸⁻⁴⁰ and it entails that we solve Maxwell's equations numerically on a two-dimensional grid. We assumed the following physical characteristics:

a waveguide width of $0.4 \mu\text{m}$, a gap between the guide and the disk of width $0.25 \mu\text{m}$, a disk radius of $2.54 \mu\text{m}$, a circular particle of radius $0.25 \mu\text{m}$, and use of TM polarization (that is, \mathbf{E} perpendicular to the plane containing the guide and disk). We also assume that the guide and disk have a dielectric constant of 4.0 and are separated by vacuum; these values mimic in two dimensions the three-dimensional nature of the waveguiding. We model the absorbing particle by assuming that the real part of its dielectric constant is also 4.0 and that its absorption can be described by a conductivity of $3000 \Omega^{-1} \text{m}^{-1}$. We find from the results of our numerical simulation that these values lead to a buildup factor of 16 in the absence of the absorbing particle and a value of 3 in its presence. The results given in Fig. 5 provide independent verification of the predictions given in Section 3 that are based on the formalism developed in Section 2. This formalism is based on the fact that we attribute the phenomenological coefficients r and t to the coupling of light into and out of the disk resonator. The approach of this section is likely to prove extremely useful in the design of integrated photonic biosensors.

6. Summary

We have described the design of a sensitive biosensor based on the enhancement of the absorption of a biological material through use of optical resonance. We have presented a theoretical model of such a device and have performed an estimate of its sensitivity that suggests that it can detect as few as 100 molecules. We have also presented a simulation of the operation of this device based on a direct integration of Maxwell's equations.

This research was sponsored by the Defense Advanced Research Projects Agency under grant MDA972-00-1-0021. The content of this paper does not necessarily reflect the position or the policy of the U.S. government, and no official endorsement should be inferred. The authors thank A. S. Baca, A. Baemner, G. Baxter, J. E. Fajardo, and E. M. Nagasako for useful discussions of the optical properties of biological materials.

References and Notes

1. G. W. Christopher, T. J. Cielak, J. A. Pavlin, and E. M. Eitzen, "Biological warfare, a historical perspective," *J. Am. Med. Assoc.* **278**, 412-417 (1997).
2. J. W. Hall and A. Pollard, "Near-infrared spectrophotometry: a new dimension in clinical chemistry," *Clin. Chem. (Winston-Salem, N.C.)* **38**, 1623-1631 (1992).
3. B. J. Luff, R. D. Harris, J. S. Wilkinson, R. Wilson, and D. J. Schiffrin, "Integrated-optical directional coupler biosensor," *Opt. Lett.* **21**, 618-620 (1996).
4. B. J. Luff, J. S. Wilkinson, J. Piehler, U. Hollenbach, J. Ingenhoff, and N. Fabricius, "Integrated optical Mach-Zehnder biosensor," *J. Lightwave Technol.* **16**, 583-592 (1998).
5. W. Lukosz, "Principles and sensitivities of integrated optical and surface plasmon sensors for direct affinity sensing and immunosensing," *Biosens. Bioelectron.* **6**, 215-225 (1991).
6. A. A. Kolomenskii, P. D. Gershon, and H. A. Schuessler, "Sensitivity and detection limit of concentration and adsorption

- measurements by laser-induced surface-plasmon resonance," *Appl. Opt.* **36**, 6539–6547 (1997).
7. A. A. Kolomenskii, P. D. Gershon, and H. A. Schuessler, "Surface-plasmon resonance spectrometry and characterization of absorbing liquids," *Appl. Opt.* **39**, 3314–3320 (2000).
 8. S. L. McCall, A. F. J. Levi, R. E. Slusher, S. J. Pearton, and R. A. Logan, "Whispering-gallery mode microdisk lasers," *Appl. Phys. Lett.* **60**, 289–291 (1992).
 9. Y. Yamamoto and R. E. Slusher, "Optical processes in microcavities," *Phys. Today* **46**, 66–74 (1993).
 10. J. C. Knight, H. S. T. Driver, R. J. Hutcheon, and G. N. Robertson, "Core-resonance capillary-fiber whispering-gallery-mode laser," *Opt. Lett.* **17**, 1280–1282 (1992).
 11. J. Popp, M. H. Fields, and R. K. Chang, "Q-switching by saturable absorption in microdroplets: elastic scattering and laser emission," *Opt. Lett.* **22**, 1296–1298 (1997).
 12. S. Schiller and R. L. Byer, "High-resolution spectroscopy of whispering gallery modes in large dielectric spheres," *Opt. Lett.* **16**, 1138–1140 (1991).
 13. V. V. Vassiliev, V. L. Velichansky, V. S. Ilchenko, M. L. Gorodetsky, L. Hollberg, and A. V. Yarovitsky, "Narrow-line-width diode laser with a high-Q microsphere resonator," *Opt. Commun.* **158**, 305–312 (1998).
 14. B. E. Little, S. T. Chu, H. A. Haus, J. Foresi, and J.-P. Laine, "Microring resonator channel dropping filters," *J. Lightwave Technol.* **15**, 998–1005 (1997).
 15. C. K. Madsen and G. Lenz, "Optical all-pass filters for phase response design with applications for dispersion compensation," *IEEE Photon. Technol. Lett.* **10**, 994–996 (1998).
 16. V. B. Braginsky, M. L. Gorodetsky, and V. S. Ilchenko, "Quality-factor and nonlinear properties of optical whispering-gallery modes," *Phys. Lett. A* **137**, 393–397 (1989).
 17. F. C. Blom, D. R. van Dijk, H. J. Hoekstra, A. Driessen, and Th. J. A. Popma, "Experimental study of integrated-optics microcavity resonators: toward an all-optical switching device," *Appl. Phys. Lett.* **71**, 747–749 (1997).
 18. R. E. Benner, P. W. Barber, J. F. Owen, and R. K. Chang, "Observation of structure resonances in the fluorescence spectra from microspheres," *Phys. Rev. Lett.* **44**, 475–478 (1980).
 19. A. J. Campillo, J. D. Eversole, and H.-B. Lin, "Cavity quantum electrodynamic enhancement of stimulated emission in microdroplets," *Phys. Rev. Lett.* **67**, 437–440 (1991).
 20. D. W. Vernooy, V. S. Ilchenko, H. Mabuchi, E. W. Streed, and H. J. Kimble, "High-Q measurements of fused-silica microspheres in the near infrared," *Opt. Lett.* **23**, 247–249 (1998).
 21. S. Blair and Y. Chen, "Resonant-enhanced evanescent-wave fluorescence biosensing with cylindrical optical cavities," *Appl. Opt.* **40**, 570–582 (2001).
 22. L. Rayleigh, "The problem of the whispering gallery," *Philos. Mag.* **20**, 1001–1004 (1910).
 23. V. B. Braginsky and V. S. Ilchenko, "Properties of optical dielectric microresonators," *Sov. Phys. Dokl.* **32**, 306–307 (1987).
 24. Note that, in the absence of absorption, the buildup factor B is related to the finesse \mathcal{F} often used to describe optical resonators through the relation $B = (2/\pi)\mathcal{F}$.
 25. M. L. Gorodetsky, A. A. Savchenkov, and V. S. Ilchenko, "Ultimate Q of optical microsphere resonators," *Opt. Lett.* **21**, 453–455 (1996).
 26. D. Rafizadeh, J. P. Zhang, S. C. Hagness, A. Taflove, K. A. Stair, S. T. Ho, and R. C. Tiberio, "Waveguide-coupled AlGaAs/GaAs microcavity ring and disk resonators with high finesse and 21.6-nm free spectral range," *Opt. Lett.* **22**, 1244–1246 (1997).
 27. S. Arnold, C. T. Liu, W. B. Whitten, and J. M. Ramsey, "Room-temperature microparticle-based persistent spectral hole burning memory," *Opt. Lett.* **16**, 420–422 (1991).
 28. N. Dubreuil, J. C. Knight, D. K. Leventhal, V. Sandoghdar, J. Hare, and V. Lefevre, "Eroded monomode optical fiber for whispering-gallery mode excitation in fused-silica microspheres," *Opt. Lett.* **20**, 813–815 (1995).
 29. J.-P. Laine, B. E. Little, and H. A. Haus, "Etch-eroded fiber coupler for whispering-gallery-mode excitation in high-Q silica microspheres," *IEEE Photon. Technol. Lett.* **11**, 1429–1430 (1999).
 30. M. Cai, O. Painter, and K. Vahala, "Observation of critical coupling in a fiber taper to a silica-microsphere whispering-gallery mode system," *Phys. Rev. Lett.* **85**, 74–77 (2000).
 31. B. E. Little and S. T. Chu, "Toward very large-scale integrated photonics," *Opt. Photon. News* **11**, 24–29 (2000).
 32. B. L. N. Salmaso, G. J. Puppels, P. J. Caspers, R. Floris, R. Wever, and J. Greve, "Resonance Raman microspectroscopic characterization of eosinophilic peroxidase in human eosinophilic granulocytes," *Biophys. J.* **67**, 436–446 (1994).
 33. J. E. Heebner and R. W. Boyd, "Enhanced all-optical switching by use of a nonlinear fiber ring resonator," *Opt. Lett.* **24**, 847–849 (1999).
 34. B. E. Little and S. T. Chu, "Estimating surface-roughness loss and output coupling in microdisk resonators," *Opt. Lett.* **21**, 1390–1392 (1996).
 35. C. A. Rowe, L. M. Tender, M. K. Feldstein, J. P. Golden, S. B. Scroggs, B. D. MacCraith, J. J. Cras, and F. S. Ligler, "Array biosensor for simultaneous identification of bacterial, viral, and protein analytes," *Anal. Chem.* **71**, 3846–3852 (1999).
 36. We obtained the value $\sigma = 2 \times 10^{-16} \text{ cm}^2$ by converting the measured value of the optical density to an absorption cross section. See H. G. Schulze, L. S. Greek, C. J. Barbosa, M. W. Blades, B. B. Gorzalka, and R. F. B. Turner, "Measurement of some small molecule and peptide neurotransmitters in-vitro using a fiber-optics probe with pulsed ultraviolet resonance Raman spectroscopy," *J. Neurosci. Methods* **92**, 15–24 (1999). These authors measure an optical density of the order of 0.5 at a wavelength of 205 nm for a 1-cm path length through a 10- μM solution of dopamine. An optical density of 0.5 implies that the quantity αL is of the order of unity, where α is the absorption cross section and L is the path length, or that α is of the order of 1/cm. The absorption coefficient can be represented as $\alpha = N\sigma$, where N is the molecular number density and σ is the absorption cross section. Recall that a 1-M solution contains 6×10^{23} molecules/l, or 6×10^{20} molecules/ml. Thus a 10- μM solution contains 6×10^{15} molecules/ml or a number density of molecules of $N = 6 \times 10^{15} \text{ cm}^{-3}$. The molecular absorption cross section is thus given by $\sigma = 2 \times 10^{-16} \text{ cm}^2$ for dopamine.
 37. It should be noted that buildup factors as large as 10^9 have been observed, although in geometries less complicated than that of the proposed biosensor. See, for example, Ref. 25.
 38. K. S. Yee, "Numerical solution of initial boundary value problems involving Maxwell's equations in isotropic media," *IEEE Trans. Antennas Propag.* **14**, 302–307 (1966).
 39. A. Taflove and S. C. Hagness, *Computational Electrodynamics, The Finite-Difference Time-Domain Method* (Artech House, Boston, Mass., 2000).
 40. S. C. Hagness, D. Rafizadeh, S. T. Ho, and A. Taflove, "FDTD microcavity simulations: design and experimental realization of waveguide-coupled single-mode ring and whispering-gallery-mode disk resonators," *J. Lightwave Technol.* **15**, 2154–2165 (1997).